

1 **Title**

2 In vivo fascicle length measurements via B-mode ultrasound imaging with single vs
3 dual transducer arrangements

4

5 **Authors & Affiliations**

6 Scott F Brennan¹, Andrew G Cresswell¹, Dominic J Farris¹, Glen A Lichtwark¹

7

8 ¹School of Human Movement & Nutrition Sciences, The University of Queensland,
9 Brisbane, QLD, Australia, 4072.

10

11 **Corresponding author**

12 Scott F Brennan

13 School of Human Movement & Nutrition Sciences

14 E: s.brennan@uq.edu.au

15 P: (+61) 7 3365 6482

16 Fax: (+61) 7 3365 6877

17

18 **Keywords**

19 Ultrasound, muscle, fascicle, length, tracking

20

21 Abstract: 248 words

22 Main document: 2000 words

23

24 **Abstract**

25 Ultrasonography is a useful technique to study muscle contractions in vivo, however
26 larger muscles like the vastus lateralis may be difficult to visualise with smaller,
27 commonly used transducers. Fascicle length is often estimated using linear
28 trigonometry to extrapolate fascicle length to regions where the fascicle is not visible.
29 However, this approach has not been compared to measurements made with a larger
30 field of view for dynamic muscle contractions. Here we compared two different single-
31 transducer extrapolation methods to measure VL muscle fascicle length to a direct
32 measurement made using two synchronised, in-series transducers. The extrapolation
33 methods used either pennation angle and muscle thickness to extrapolate fascicle
34 length outside the image (extrapolate method) or determined fascicle length based on
35 the extrapolated intercept between fascicle and aponeurosis (intercept method). Nine
36 participants performed maximal effort, isometric, knee extension contractions on a
37 dynamometer at 10° increments from 50-100° of knee flexion. Fascicle length and
38 torque were simultaneously recorded for offline analysis. The dual transducer method
39 showed similar patterns of fascicle length change (overall mean coefficient of multiple
40 correlation was 0.76 and 0.71 compared to extrapolate and intercept methods
41 respectively), but reached different absolute lengths during the contractions. This had
42 the effect of producing force-length curves of the same shape, but each curve was
43 shifted in terms of absolute length. We concluded that dual transducers are beneficial
44 for studies that examine absolute fascicle lengths, whereas either of the single
45 transducer methods may produce similar results for normalised length changes, and
46 repeated measures experimental designs.

47

48

49 **Introduction**

50 Ultrasonography allows for non-invasive measurement of muscle fascicle geometry
51 during muscle contractions. For human muscles with relatively short fascicles, like
52 *gastrocnemius* or *tibialis anterior*, dynamic imaging is relatively simple because the
53 majority of the muscle fascicle is visible within the field of view (FOV) of the transducer
54 (Brennan et al., 2017; Cronin et al., 2013; Day et al., 2013; Kawakami et al., 1998;
55 Maganaris, 2003). Measurements of longer fascicles in muscles like *vastus lateralis*
56 (VL) are more difficult due to the required FOV being larger.

57

58 Different methods are available to overcome the FOV issue. The first method is to use
59 a longer transducer that can image a larger FOV (Sharifnezhad et al., 2014).
60 However, longer transducers (e.g. 10 cm) often have a limited frame rate because of
61 the greater time it takes to obtain data along the length of the transducer, and can
62 have reduced image quality depending on the number of crystal elements per unit
63 length. Another method is to use extended FOV techniques (Noorkoiv et al., 2010),
64 which is a valid and reliable method for static measurements when there are not
65 changes in muscle force and/or fascicle length. The most common method to
66 overcome FOV issues during dynamic contractions is to use linear trigonometry to
67 estimate the length of the portion of the fascicle that is outside the FOV of a single
68 transducer (Austin et al., 2010; Finni et al., 2003; Fontana et al., 2014). An alternative
69 is to utilise a second, in-series transducer to simultaneously record images of the part
70 of the fascicle not visible by the first transducer (Bolsterlee et al., 2016; 2015; Herbert
71 et al., 2011; 2015). Using a second transducer, both fascicle endpoints are visible,
72 reducing some of the uncertainty in fascicle length measurements. For dynamic

73 fascicle tracking, estimations of fascicle length from a single transducer have not yet
74 been compared to length measurements from a greater FOV using two transducers.

75

76 The aim of the study was to determine if dynamic measurements of VL fascicle length
77 using extrapolation methods with one transducer during isometric knee extension
78 contractions match those made with two synchronised, in-series transducers. We
79 hypothesised that the absolute lengths of the fascicles would differ between the single
80 and dual ultrasound techniques, due to the ability to visualise the fascicle endpoint.
81 However, we also predicted that any differences would be negligible for normalised
82 length changes, and hence, would not affect observations made using a repeated
83 measures design.

84

85 **Methods**

86 **Protocol**

87 Nine participants (age 26 ± 2.5 years, mass 72.8 ± 7.0 kg, height 178 ± 6.3 cm)
88 provided informed consent to participate in the study. The study was approved by an
89 institutional ethics committee. Each participant completed maximal effort, isometric,
90 knee extension contractions on an isokinetic dynamometer (HUMAC NORM, CSMi
91 Inc., Stoughton, MA, USA). A familiarisation session was completed to make sure that
92 they could perform consistent maximal efforts. A second experimental session
93 followed within 10 days, which included the ultrasound measurements. The two
94 sessions used the same protocol and dynamometer position.

95

96 Participants were seated in the dynamometer with a hip angle of 80° and the
97 dynamometer attachment adjusted to align with the flexion/extension axis of the left

98 knee. A 60-s isotonic warm up protocol was performed using the interactive path
99 program on the dynamometer. The isometric protocol consisted of randomised blocks
100 of three maximal effort, isometric contractions at 10⁰ increments from 50⁰-100⁰ of knee
101 flexion. A straight leg was defined as 0⁰ of knee flexion. For each contraction
102 participants were instructed to perform a ramp contraction to maximal effort over a 3-
103 s period, and hold the maximum effort for 1-s before relaxing. Two minutes rest was
104 given between trials to avoid any potential fatigue effects.

105

106 **Dynamometer measurements**

107 Knee extensor torque and joint angle were sampled from the analogue output of the
108 dynamometer using a CED Micro 1401 A/D converter at a 2kHz sample rate and
109 recorded in Spike 2 software (Cambridge Electronic Design Ltd., Cambridge,
110 England). The torque signal was filtered using a 10 Hz, first-order, low-pass, bi-
111 directional Butterworth filter in Matlab (MathWorks Inc., Natick, MA, USA). The
112 maximum gravity effective torque (maxGET) was taken as the resting torque with the
113 knee at full extension (0⁰). Torque was then gravity corrected using maxGET and joint
114 angle (Pincivero et al., 2004; Westing and Seger, 1989). Passive torque was
115 calculated as the difference between the resting torque and gravity corrected torque
116 prior to the contraction. The best two-out-of-three trials based on maximal torque were
117 analysed for each joint angle.

118

119 **Ultrasound measurements**

120 Muscle fascicle measurements of VL were made using two flat ultrasound transducers
121 (LV7.5/60/96Z, TELEMED, Vilnius, Lithuania) that were held end-to-end by a custom
122 made frame (Figure 1). Due to the shape of the transducer, there was a 22 mm gap

123 between the visual fields of the transducers. A custom Matlab script was written to
124 'stitch' the images together (Figure 1c). The transducers were placed at approximately
125 50% thigh length, following a line between the greater trochanter and superior patella
126 insertion. A self-adhesive compression bandage was used to secure the transducers
127 to the thigh. The central frequency of the transducer was set at 5 MHz, image depth
128 at 50 mm, and sampling rate of 80 Hz. A logic pulse from the first ultrasound system
129 triggered data capture by the other system, which produced its own logic pulse. The
130 two pulses were recorded by the A/D board to determine any delay between the onsets
131 of image collection. A semi-automated tracking algorithm (Cronin et al., 2011; Farris
132 and Lichtwark, 2016; Gillett et al., 2013) tracked the positions of the visible fascicle,
133 and the deep and superficial aponeuroses, which was subsequently used to estimate
134 fascicle length using three different methods.

135

136 **Method 1** - *Extrapolation*

137 Fascicle length for the "extrapolation" method (Figure 1a) was calculated from the
138 proximal image using the equation:

139

$$140 \quad FL = \text{visible fascicle length} + h/\sin(PA)$$

141

142 where 'h' equals the vertical distance between the intersection of the visible fascicle
143 with the image border and the deep aponeurosis; and PA equals the pennation angle
144 of the tracked fascicle (Austin et al., 2010; Finni et al., 2003; Fontana et al., 2014).

145 **Method 2** - *Intercept*

146 Fascicle length for the "intercept" method (Figure 1b) was calculated from the proximal
147 image using:

148

149 $FL = \text{visible fascicle length} + \text{predicted length}$

150

151 where the predicted length is equal to the distance between the visible fascicle's
152 intersection with the image border and the intersection of the linearly extrapolated
153 paths of the visible fascicle and deep aponeurosis (Blazevich et al., 2009).

154 **Method 3** – *Dual*

155 The proximal and distal images of VL were used to separately track the positions of
156 the proximal and distal endpoints of a line assumed to be representative of a single
157 fascicle (Figure 1c). The proximal insertion and visible fascicle length was defined first,
158 then the distal 'fascicle' was defined as the continuation of that line within the distal
159 image. Fascicle lengths were calculated as the distance between the origin of the
160 fascicle in the proximal image and the distal intersection with the deep aponeuroses
161 in the distal image.

162

163 Due to the large proportion of fascicle length that is estimated, Methods 1 and 2
164 (extrapolate and intercept) are highly sensitive to changes in the orientation of the
165 deep aponeurosis. As such, the coordinates of the tracking points were filtered using
166 a 5 Hz, second-order, low-pass, bi-directional, Butterworth filter to reduce the chances
167 of non-physiological length changes as a result of the calculations. Fascicle lengths
168 were then calculated from the filtered X-Y coordinates and interpolated to the analogue
169 sampling rate.

170

171 **Analysis**

172 Quadriceps force was calculated as active torque divided by the angle specific VL
173 moment arm, **calculated individually using a modified *gait 2392* musculoskeletal model**
174 **in OpenSim software and standard scaling procedures** (Delp et al., 1990). **The scale**
175 **factors were determined from markers placed on anatomical landmarks of the pelvis**
176 **and left lower limb.** Fascicle length was recorded at rest and at the time of maximal
177 quadriceps force for each contraction at each joint position. The change in fascicle
178 length from the resting state to maximum quadriceps force was also calculated.

179

180 For each individual a force-length curve was fitted, based on physiologically
181 appropriate models (Azizi and Roberts, 2010)

$$182 \quad F_{active} = e^{-|(L^b-1)/s|^\alpha}$$

183

184 where F is force, L is fascicle length, a is roundness, b is skewness, and s is width.
185 The curve fit was optimised using a nonlinear least squares method.

186

187 A coefficient of multiple correlation (CMC) analysis was performed for each joint angle,
188 comparing the waveform fascicle lengths of Method 3 with each of the other estimation
189 methods, averaged across two trials. A two-way repeated measures ANOVA (method
190 x joint angle) was performed on fascicle length and fascicle length change data, with
191 Dunnett's multiple comparisons where interactions were found. **A one-way repeated**
192 **measures ANOVA was used to compare L_0 across methods.** The coefficient of
193 variation (R^2) of the force-length fits was calculated to measure how well the curve fit
194 explained the variance in the data. An alpha level of 0.05 was used for all statistical
195 tests. Values in text are shown as mean \pm standard deviation (SD).

196

197 **Results**

198 CMC's between the dual transducer method and the two single transducer methods
199 showed that the pattern of fascicle length changes was consistent across methods
200 (Table 1, Figure 2a). The extrapolate method had higher CMC values at shorter
201 lengths (smaller joint angle) and lower CMC values at longer lengths, whereas the
202 intercept method was consistent across joint angles. The pattern of fascicle length
203 changes had consistent temporal phases across methods, with high values for CMCs
204 (Table 1, Figure 2a), but the absolute fascicle length range varied between methods
205 (Figure 2b).

206

207 There was a significant main effect of method on fascicle shortening ($F = 28.71$, $p <$
208 0.01), with no significant interaction ($F = 1.52$, $p = 0.15$, Figure 3b). The extrapolate
209 and intercept methods showed greater fascicle shortening compared to the dual
210 transducer method by a mean of 24.64 mm (95% CI = 16.75 – 32.53) and 11.38 mm
211 (95% CI = 3.49 – 19.27) respectively across all joint angles.

212

213 The dual transducer method (106 ± 10 mm) predicted the largest L_o , where both the
214 intercept (90 ± 17 mm) and the extrapolation (89 ± 16 mm) resulted in a significantly
215 lower predicted L_o ($F = 18.7$, $p < 0.01$). The normalised force-length curves for each
216 of the methods are shown in Figure 4. The R-squared values for the extrapolation,
217 intercept and dual transducer curve fits were 0.72 ± 0.14 , 0.72 ± 0.13 , and 0.74 ± 0.10
218 respectively.

219

220 **Discussion**

221 The main findings of the study suggest that fascicle length measurements made by
222 the different methods result in absolute differences in fascicle length. However, these
223 differences appear to be systematic and the pattern of length change between the
224 different methods is consistent. Furthermore, the effect on normalised lengths is
225 minimal.

226

227 We observed that a second ultrasound transducer is beneficial for visualising the distal
228 changes in muscle orientation. The greater fascicle shortening and shorter fascicle
229 lengths at maximal force in both of the single transducer methods may be due to
230 underestimation of fascicle length by tracking only the proximal region of the muscle.
231 The greater shortening resulted in lower predicted absolute L_o values, however that
232 shift was not evident when utilising normalised fascicle lengths (Figure 4). Therefore,
233 if understanding absolute fascicle lengths is important, using a second ultrasound
234 transducer to visualise the distal fascicle endpoint is recommended. The use of either
235 single transducer method would provide similar results for experimental data
236 measuring differences in muscle contraction dynamics within-participants. Thus, for a
237 repeated measures design, the choice of estimation method may shift the overall data
238 set but not alter the effects of experimental factors.

239

240 *Limitations*

241 We assumed that a second transducer is beneficial because it is possible to visualise
242 the distal muscle region. However, the dual transducer method used in this study was
243 not validated against any other fascicle measurement technique such as diffusion
244 tensor imaging (Bolsterlee et al., 2015) or extended FOV techniques (Noorkoiv et al.,

245 2010) because there is not currently a gold standard measurement for dynamic muscle
246 contractions.

247

248 **Conflict of Interest Statement**

249 The authors have no conflict of interest to disclose.

250

251 **Funding**

252 Scott Brennan is supported by an Australian Postgraduate Award scholarship. There
253 were no external sponsors providing financial support for the study.

254

255

256 **References**

257

258 Austin, N., Nilwik, R., Herzog, W., 2010. In vivo operational fascicle lengths of vastus

259 lateralis during sub-maximal and maximal cycling. *Journal of Biomechanics*. 43,

260 2394–2399.

261 Azizi, E., Roberts, T.J., 2010. Muscle performance during frog jumping: influence of

262 elasticity on muscle operating lengths. *Proceedings of the Royal Society B:*

263 *Biological Sciences*. 277, 1523–1530.

264 Blazevich, A.J., Coleman, D.R., Horne, S., Cannavan, D., 2009. Anatomical predictors

265 of maximum isometric and concentric knee extensor moment. *European Journal*

266 *of Applied Physiology*. 105, 869–878.

267 Bolsterlee, B., Gandevia, S.C., Herbert, R.D., 2016. Effect of transducer orientation on

268 errors in ultrasound image-based measurements of human medial gastrocnemius

269 muscle fascicle length and pennation. *PLoS ONE*. 11, e0157273.

270 Bolsterlee, B., Veeger, H.E.J.D., van der Helm, F.C.T., Gandevia, S.C., Herbert, R.D.,

271 2015. Comparison of measurements of medial gastrocnemius architectural

272 parameters from ultrasound and diffusion tensor images. *Journal of Biomechanics*.

273 48, 1133–1140.

274 Brennan, S.F., Cresswell, A.G., Farris, D.J., Lichtwark, G.A., 2017. The effect of

275 cadence on the muscle-tendon mechanics of the gastrocnemius muscle during

276 walking. *Scandinavian Journal of Medicine & Science in Sports*. 27, 289–298.

277 Cronin, N.J., Avela, J., Finni, T., Peltonen, J., 2013. Differences in contractile

278 behaviour between the soleus and medial gastrocnemius muscles during human

279 walking. *Journal of Experimental Biology*. 216, 909–914.

280 Cronin, N.J., Carty, C.P., Barrett, R.S., Lichtwark, G., 2011. Automatic tracking of

281 medial gastrocnemius fascicle length during human locomotion. *Journal of Applied*

282 Physiology. 111, 1491–1496.

283 Day, J.T., Lichtwark, G.A., Cresswell, A.G., 2013. Tibialis anterior muscle fascicle
284 dynamics adequately represent postural sway during standing balance. *Journal of*
285 *Applied Physiology*. 115, 1742–1750.

286 Delp, S.L., Loan, J.P., Hoy, M.G., Zajac, F.E., Topp, E.L., Rosen, J.M., 1990. An
287 interactive graphics-based model of the lower extremity to study orthopaedic
288 surgical procedures. *IEEE Transactions on Biomedical Engineering*. 37, 757–767.

289 Farris, D.J., Lichtwark, G.A., 2016. UltraTrack: Software for semi-automated tracking
290 of muscle fascicles in sequences of B-mode ultrasound images. *Computer*
291 *Methods and Programs in Biomedicine*. 128, 111–118.

292 Finni, T., Ikegawa, S., Lepola, V., Komi, P.V., 2003. Comparison of force-velocity
293 relationships of vastus lateralis muscle in isokinetic and in stretch-shortening cycle
294 exercises. *Acta Physiologica Scandinavica* 177, 483–491.

295 Fontana, H. de B., Roesler, H., Herzog, W., 2014. In vivo vastus lateralis force-velocity
296 relationship at the fascicle and muscle tendon unit level. *Journal of*
297 *Electromyography & Kinesiology*. 24, 934–940.

298 Gillett, J.G., Barrett, R.S., Lichtwark, G.A., 2013. Reliability and accuracy of an
299 automated tracking algorithm to measure controlled passive and active muscle
300 fascicle length changes from ultrasound. *Computer Methods in Biomechanics and*
301 *Biomedical Engineering*. 16, 678–687.

302 Herbert, R.D., Clarke, J., Kwah, L.K., Diong, J., Martin, J., Clarke, E.C., Bilston, L.E.,
303 Gandevia, S.C., 2011. In vivo passive mechanical behaviour of muscle fascicles
304 and tendons in human gastrocnemius muscle-tendon units. *Journal of Physiology*.
305 589, 5257–5267.

306 Herbert, R.D., Héroux, M.E., Diong, J., Bilston, L.E., Gandevia, S.C., Lichtwark, G.A.,

307 2015. Changes in the length and three-dimensional orientation of muscle fascicles
308 and aponeuroses with passive length changes in human gastrocnemius muscles.
309 *Journal of Physiology*. 593, 441–455.

310 Kawakami, Y., Ichinose, Y., Fukunaga, T., 1998. Architectural and functional features
311 of human triceps surae muscles during contraction. *Journal of Applied Physiology*.
312 85, 398–404.

313 Maganaris, C.N., 2003. Force-length characteristics of the in vivo human
314 gastrocnemius muscle. *Clinical Anatomy*. 16, 215–223.

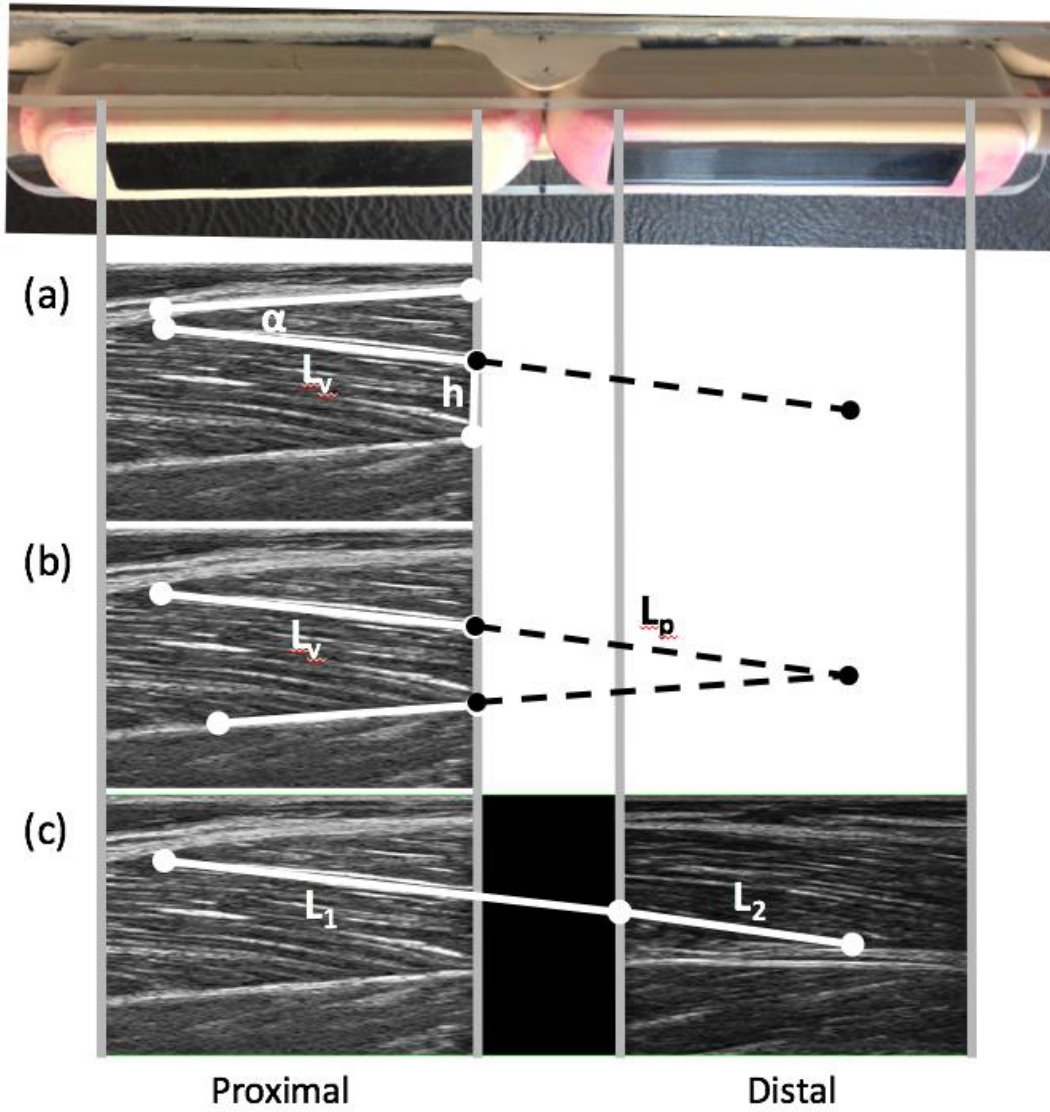
315 Noorkoiv, M., Stavnsbo, A., Aagaard, P., Blazevich, A.J., 2010. In vivo assessment of
316 muscle fascicle length by extended field-of-view ultrasonography. *Journal of*
317 *Applied Physiology*. 109, 1974–1979.

318 Pincivero, D.M., Salfetnikov, Y., Campy, R.M., Coelho, A.J., 2004. Angle- and gender-
319 specific quadriceps femoris muscle recruitment and knee extensor torque. *Journal*
320 *of Biomechanics*. 37, 1689–1697.

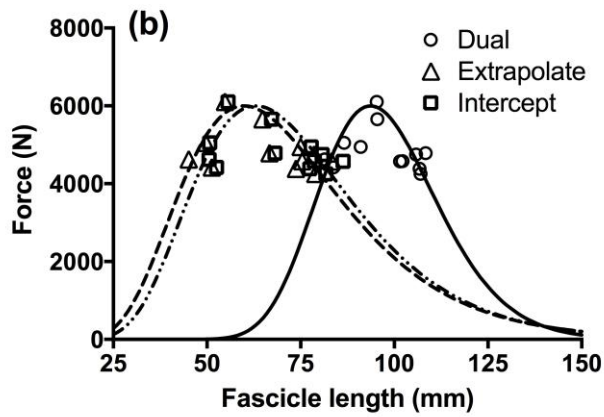
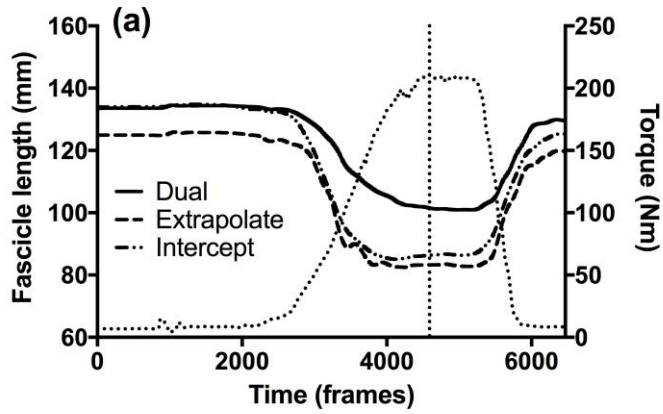
321 Sharifnezhad, A., Marzilger, R., Arampatzis, A., 2014. Effects of load magnitude,
322 muscle length and velocity during eccentric chronic loading on the longitudinal
323 growth of the vastus lateralis muscle. *Journal of Experimental Biology*. 217, 2726–
324 2733.

325 Westing, S.H., Seger, J.Y., 1989. Eccentric and concentric torque-velocity
326 characteristics, torque output comparisons, and gravity effect torque corrections
327 for the quadriceps and hamstring muscles in females. *International Journal of*
328 *Sports Medicine*. 10, 175–180.

329
330
331
332
333
334



335
 336
 337
 338



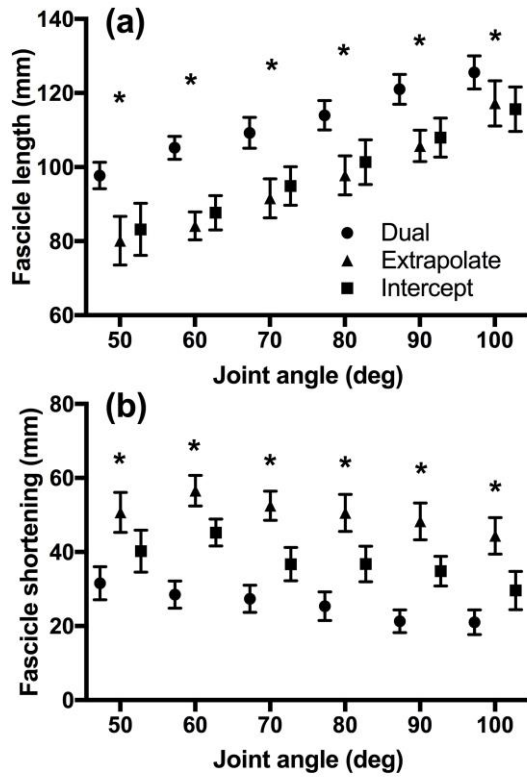
339
340
341

Joint Angle	Extrapolate	Intercept
50	0.80 ± 0.17	0.75 ± 0.17
60	0.80 ± 0.12	0.77 ± 0.07
70	0.76 ± 0.12	0.67 ± 0.20
80	0.77 ± 0.11	0.72 ± 0.15
90	0.77 ± 0.09	0.65 ± 0.25
100	0.66 ± 0.16	0.69 ± 0.21

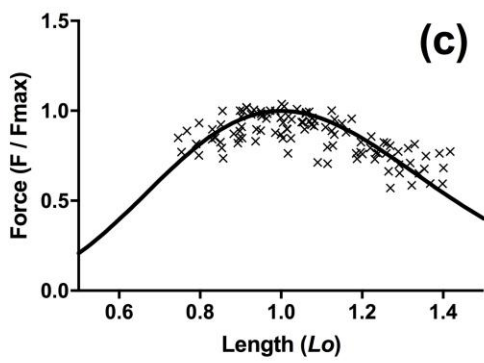
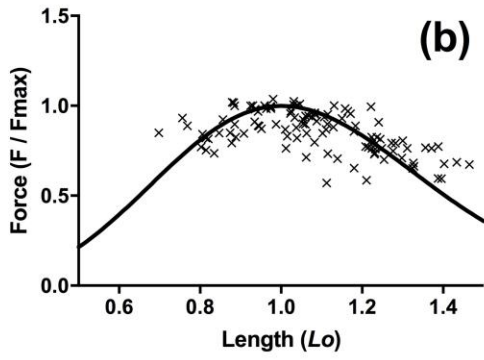
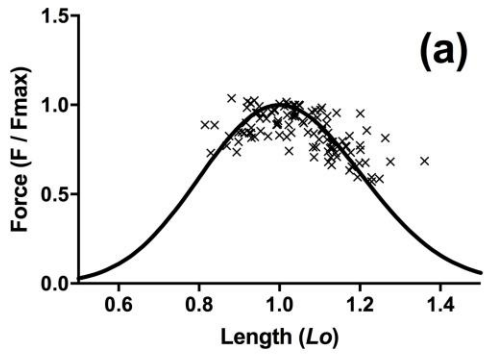
342
343
344

Coefficient	Extrapolate	Intercept	Dual
b	0.38 ± 0.65	0.42 ± 0.70	0.74 ± 0.97
s	0.20 ± 0.35	0.25 ± 0.43	0.20 ± 0.25

345
346



347



348

349

350 **Figure 1.** Schematic of the different methods of estimating fascicle length in the vastus
351 lateralis muscle. The top of the image shows the frame used to hold the two ultrasound
352 transducers. The extrapolate method (a) and intercept method (b) use only the information
353 from the proximal transducer, whereas the dual transducer method (c) uses two separate
354 fields of view. The extrapolate method calculates the remaining portion of the muscle fascicle
355 by dividing the remaining muscle thickness (h) by the sine of the pennation angle (α). The
356 intercept method calculates the remaining portion of the muscle fascicle length by finding the
357 intersection of the extrapolated paths of the visible fascicle and deep aponeuroses, each
358 defined by a respective linear equation $y=mx+c$. The dual transducer method uses
359 information from both regions of interest (red dashed lines) to track the movement of two
360 parts of a visible fascicle (L_1 & L_2).

361
362 **Figure 2.** Example data from a representative subject, showing the patterns of fascicle
363 length change (a) and force-length curves (b) for each method. (a) Torque is plotted
364 against the right axis (dotted). The vertical line indicates the occurrence of peak torque
365 development and the point at which fascicle length measurements were taken during the
366 trial. (b) The absolute force-length curves show that the curves are the same shape but
367 fascicle length ranges vary across methods. The line types in (b) match the legend from
368 (a).

369
370 **Table 1.** Coefficient of multiple correlation (CMC) values for extrapolate and intercept
371 methods compared to the dual transducer method. Data are shown as group mean \pm SD.

372
373 **Table 2.** Curve fit coefficients for the three different length estimation methods. Data are
374 shown as group mean \pm SD.

375
376 **Figure 3.** Fascicle length at maximum force (a) and fascicle shortening (b) determined by
377 each of the three different methods. Data are shown as group mean \pm SE. Annotations
378 show significant differences between all groups at the relevant joint angle.

379
380 **Figure 4.** Force-length curves of the normalised data for the dual transducer method (a), the
381 intercept method (b), and extrapolate method (c). Each point represents a data point on an
382 individual force-length curve, normalised to the respective F_{max} and L_o . The curve fits
383 represent a new fit of the normalised data points for each method.

384

